VERIFICATION OF LAMINATE COMPOSITE PLATE SIMULATION UNDER COMBINED LOADINGS THERMAL STRESSES

Prof. Dr.Nabeel K. Abid AL-sahib
University of Baghdad
Al-khwarzmi College of Engineering
Mechatronics Department

Asst Prof. Dr.Adnan N. Jameel
University of Baghdad
College of Engineering
Mechanical Department

Dr. Louay S. Yousuf
University of Baghdad
College of Engineering
Mechanical Department

ABSTRACT

This study deals with thermal cyclic loading phenomena of plates which were fabricated from composite materials (woven roving fiber glass + polyester) were exposed to (75 C°) temperature gradient thermal shock for ten times in different stage of conditioning times due to the effect of thermal fatigue using the method of Levy solution and compared these results with both results from experimental published work and (ANSYS Ver. 9) program. A composite laminate plate with fiber volume fraction (υ_f =25.076%) is selected in this study and applying the combined loadings like bending moment (Mo), and in-plane force (Nxx) beside the effect of thermal fatigue. It involves multi theoretical and finite element fields; but the theoretical one contains the derived equation of stresses distribution and evaluating the normal deflection of a middle point for dynamic analysis applying different boundary conditions for heating and cooling. The main present numerical results for a composite plate with (80%) fiber volume fraction claim that the relative reduction in normal deflection and dynamic load factor are (78.593%) and (9.421%) during cooling to (-15 $^{\circ}C$) respectively.

الخلاصة:

هذه الدراسة تتناول ظاهرة التحميل الحراري الدوري للصفائح التي كانت مصنعة من المواد المركبة (ألياف زجاجية + بوليستر) والمعرضة الى انحدار حراري بصدمة حرارية بمقدار (75) درجة سليزية لعشر دورات من مراحل وقت العمل نتيجة لتاثير الكلال الحراري باستخدام طريقة ليفي ومقارنة هذه النتائج مع كلا من نتائج برنامج الانسيز ذات الطبعة التاسعة ونتائج بحث عملي منشور مسبقا. ان الصفيحة الرقائقية المركبة بكسر حجمي (25.076%) تم اختيارها في هذه الدراسة بعد تطبيق الاحمال المركبة مثل عزم الانحناء وقوة الانضغاط الى جانب التحميل الحراري الدوري. ويتضمن هذا العمل عدة جوانب نظرية وعددية ، حيث يشمل الجانب النظري اشتقاق معادلات توزيع الاجهادات وتقييم الانحراف العمودي في نقطة المنتصف للتحليلات الديناميكية مع تطبيق شروط حدية

مختلفة في حالتي التسخين والتبريد. إن أداء النتائج العددية الرئيسية الحالية للمادة المركبة مع كسر حجمي (80%) يؤدي إلى انخفاض نسبي بالانحراف العمودي وعامل الحمل الديناميكي بنسب (78.593%) و (9.421%) نتيجة التبريد إلى (-15 درجة مئوية) على التوالي.

KEY WORD: thermal stress, composite laminate, dynamic analysis, plate simulation, combined loadings.

INTRODUCTION

Many researches before studied the effect of thermal fatigue in woven roving glass fibers with unsaturated polyester composite plate and its application on airspace experimentally. The effect of thermal cycles on tensile properties and coefficient of thermal expansion has been studied on graphite-epoxy 12-ply laminate configuration subjected to 5000 thermal cycles, [Fabmy A.A. and Cunningbam T.G., 1976]; but the method prediction applied on T300 graphite/934 epoxy under hygro-thermo-mechanical fatigue with two step procedure. The initial step consists of determining the composite ply strength associated with each type of cyclic load: mechanical, thermal and hygral. The next step is to determine the effect of combined cyclic loading [Ginty C.A. and Chamis C.C., 1988]. It can be estimate the inter-laminar shear strength (ILSS) of glass/epoxy and glass/polyester composites of woven fabrics by changing the holding time at the holding temperature during the thermal fatigue and hydrothermal shock cycles [Ray B.C., 2005]. In the other hand the inter-laminar shear strength (ILSS) of the thermally conditioned glass fibers of random orientation and epoxy resin laminates followed by ice-cold water quenching from the laminated composite was exposed to (50˚C) temperature and hydrothermal fatigue cycles varied weight fraction constituents of glass fiber reinforced (55,60, 65%), [Ray B.C., 2005], but in the field of cryogenic [Ray B.C., 2005] studied the effect for 55,60, and 65 weight percentages of E-glass fibers reinforced epoxy composites on inter-laminar shear strength during (sub-ambient) at -80˚C temperature in ultra low freezing chamber for 2 hours and subjected to an ambient at 30˚C temperature for 1 hour and investigate the effect of thermal shock on flexural modulus of Kevlar 49/epoxy laminates by thermally conditioned at a (80˚C) for (5, 10, and 20 min) to (-80˚C) for (5 min) or cryogenically conditioned at (-80˚C) for the same time periods to (80˚C) for (5 min). In the present work it can study the effect of combined loadings on the deflection combining with thermal fatigue effect of composite laminate plate.

So that the objectives of this research are:

- In dynamic analysis derive the analytical solution to evaluate the stress-strain field and inter-laminar shear stress (ILSS) distributions for middle point using Levy solution for thermal cyclic under combined loadings.
- It will be compared the results of deflection in z-direction for middle point were obtained from thermal cyclic loading only with that obtained from (cyclic thermal loading + M_o), (cyclic thermal loading +N_{xx}) and (cyclic thermal loading +$M_o + N_{xx}$) as mentioned in Fig. (1) to obtain perfect design of deflection.
- Applying different boundary conditions like (SSSS, CSSS, and CSCS) on composite plate under cyclic thermal loading.

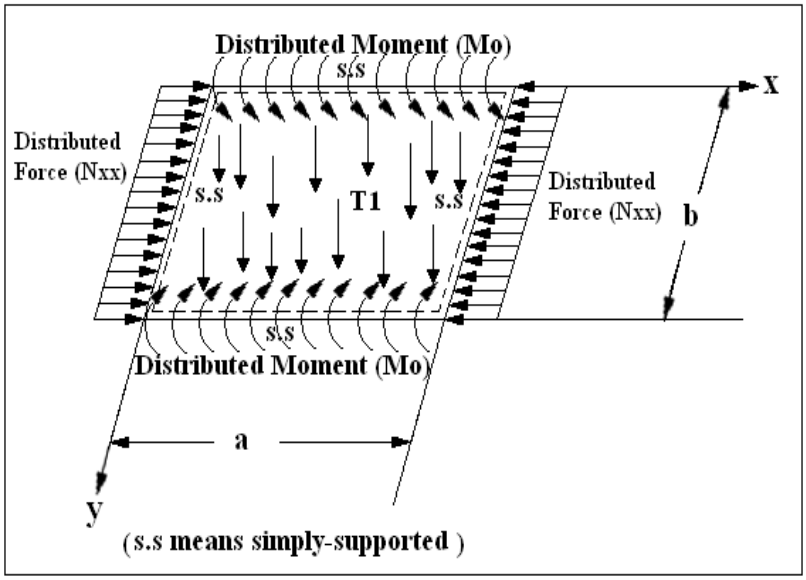

Fig. (1) Plate under thermal and combined loading.

THE CLASSICAL LAMINATED PLATE THEORY (CLPT)

The classical laminate plate theory gives flexibility than the other methods of solution for composite plate depending upon the cyclic thermal loading, in-plane force(N_{xx}), and the bending moment (M_o).

The stress and strain variation through the laminate thickness based on the classical lamination theory (CLPT) includes the following assumptions, [Reddy J.N. 2004]:

- Transverse normal stresses remain straight before and after deformation (strain in z- direction equal to zero).
- Transverse normal stresses rotate and perpendicular to the mid-surface after deformation (strain in xz and yz plane equal to zero).

DISPLACEMENTS KINETIC RELATIONS

If a plate was established of a total thickness (h) composed of (N) orthotropic layers with the principal material coordinates (x_1^k, x_2^k, x_3^k) of the *k*th lamina oriented at an angle θ_k to the laminate coordinate, *x*. The *z*-axis is taken positive downward from the mid plane. The kth layer is located between the points $z = z_k$ and $z = z_{k+1}$ in the thickness direction. The *Kirchhoff hypothesis* theory used instead of *Mendlin* theory by applying the principles of supper position displacements $(u, v, w)$to be such that, [Reddy J.N. 2004] :

$$u(x,y,z,t) = u_o(x,y,t) - z * \frac{\partial w_o}{\partial x}$$

$$v(x,y,z,t) = v_o(x,y,t) - z * \frac{\partial w_o}{\partial y} \quad (1)$$

$$w(x,y,z,t) = w_o(x,y,t)$$

Where:

(u_o, v_o, w_o) : A displacements along the coordinate lines of a materials point on the *x*,*y*-plane. The strain-displacement matrix relations take the form, [Reddy J.N. 2004]:

$$\begin{Bmatrix} \varepsilon_{xx} \\ \varepsilon_{yy} \\ \gamma_{xy} \end{Bmatrix} = \begin{Bmatrix} \varepsilon_{xx}^{(0)} \\ \varepsilon_{yy}^{(0)} \\ \gamma_{xy}^{(0)} \end{Bmatrix} + z * \begin{Bmatrix} \varepsilon_{xx}^{(1)} \\ \varepsilon_{yy}^{(1)} \\ \gamma_{xy}^{(1)} \end{Bmatrix}$$ where:

$$\{\varepsilon^{(0)}\} = \begin{Bmatrix} \varepsilon_{xx}^{(0)} \\ \varepsilon_{yy}^{(0)} \\ \gamma_{xy}^{(0)} \end{Bmatrix} = \begin{Bmatrix} \frac{\partial u_o}{\partial x} \\ \frac{\partial v_o}{\partial y} \\ \frac{\partial u_o}{\partial y} + \frac{\partial v_o}{\partial x} \end{Bmatrix} \quad (2)$$

$$\{\varepsilon^{(1)}\} = \begin{Bmatrix} \varepsilon_{xx}^{(1)} \\ \varepsilon_{yy}^{(1)} \\ \gamma_{xy}^{(1)} \end{Bmatrix} = \begin{Bmatrix} -\frac{\partial^2 w_o}{\partial x^2} \\ -\frac{\partial^2 w_o}{\partial y^2} \\ -2 * \frac{\partial^2 w_o}{\partial x \partial y} \end{Bmatrix}$$

For orthotropic material and layers axes oriented arbitrarily with respect to the laminate coordinates. The Hook's Law relations are [Reddy J.N. 2004]:

$$\{\sigma\}_k = \left[\overline{Q}\right]_k \{\varepsilon\}_k$$

$$\begin{Bmatrix}\sigma_{xx}\\ \sigma_{yy}\\ \sigma_{xy}\end{Bmatrix}^{k}=\begin{bmatrix}\bar{Q}_{11} & \bar{Q}_{12} & \bar{Q}_{16}\\ \bar{Q}_{12} & \bar{Q}_{22} & \bar{Q}_{26}\\ \bar{Q}_{16} & \bar{Q}_{26} & \bar{Q}_{66}\end{bmatrix}*\left(\begin{Bmatrix}\varepsilon_{xx}\\ \varepsilon_{yy}\\ \gamma_{xy}\end{Bmatrix}-\begin{Bmatrix}\alpha_{xx}\\ \alpha_{yy}\\ 2*\alpha_{xy}\end{Bmatrix}*\Delta T\right) \quad (3)$$

And for especially orthotropic (that the material axes coincide with respect to laminates coordinates).

$$\begin{Bmatrix}\sigma_{xx}\\ \sigma_{yy}\\ \sigma_{xy}\end{Bmatrix}^{k}=\begin{bmatrix}Q_{11} & Q_{12} & 0\\ Q_{12} & Q_{22} & 0\\ 0 & 0 & Q_{66}\end{bmatrix}*\left(\begin{Bmatrix}\varepsilon_{xx}\\ \varepsilon_{yy}\\ \gamma_{xy}\end{Bmatrix}-\begin{Bmatrix}\alpha_{1}\\ \alpha_{2}\\ 0\end{Bmatrix}*\Delta T\right) \quad (4)$$

Anyhow in Levy solution (dynamic analysis) the classical laminate plate theory (CLPT) is more suitable than other methods because it is linking the cyclic thermal loading with the combined loadings.

Methodology Discussions of Theoretical and Numerical Experiences

For thermal cyclic analysis the inputs in classical laminate plate theory program can be shown in Table (1):

Table (1) The inputs in classical laminate plate theory program.

a = 0.18 m
b = 0.1 m
x = 0.09 m
y = 0.05 m
z = 0.001667 m
h = 0.004 m
$T_1 = 7500 * \sin(\omega * t)\ \frac{^{\circ}C}{m}$ for heating
$T_1 = -1875 * \sin(\omega * t)\ \frac{^{\circ}C}{m}$ for cooling

It can be taken the algebraic sum of stress field in (x, y, z) directions and deflection in z-direction for heating and cooling. Table (2) shows the verification test for dynamic analysis under

different thermal loading of fiber volume fraction ($\upsilon_f = 0.25076\,\%$) using (Fortran 90 and ANSYS Ver. 9) programs for the plate having aspect ratio (1.8). The four types of combined loading can be used in this section: (Thermal Fatigue), (Thermal Fatigue +Mo), (Thermal Fatigue +Nxx) and (Thermal Fatigue +Mo+Nxx) as mentioned in Figure (1), used (**SHELL 132**) as given in Fig. (2). It has a three-dimensional layered shell element having in-plane and thru-thickness thermal conduction capability. The element has eight nodes with up to 32 temperature degrees of freedom at each node. The conducting shell element is applicable to a three-dimensional, steady-state or transient thermal analysis.

"SHELL 132" was switched element and to be analyzed structurally, the element should replaced by an equivalent structural element such as **" SHELL 91"**. It is used for layered application of a structural shell model up to 100 different layers. The element is defined by eight nodes having six degrees of freedom at each node: translation in the nodal x, y, and z directions and rotation in the nodal x, y, and z directions to evaluate the stress field and deflection in z-direction.

A triangular-shaped element may be formed by defining the same node number. After solving the four types of combined loadings it can be compared the last three type results with first type results to obtain the perfect design of this paper. It can be used both program of finite element analysis to find the deflection and dynamic load factor (D.L.F) which cannot applied this on different fiber volume fractions because absence the knowledge of the number of layers that gives the mass of fiber experimentally. The dynamic load factor in $(T_1 = -15\ ^\circ c)$ is higher than the dynamic load factor in $(T_1 = 60\ ^\circ c)$ because the central static deflection in $(T_1 = -15\ ^\circ c)$ is smaller than the deflection in $(T_1 = 60\ ^\circ c)$ and the percentage error is acceptable on different thermal loadings.

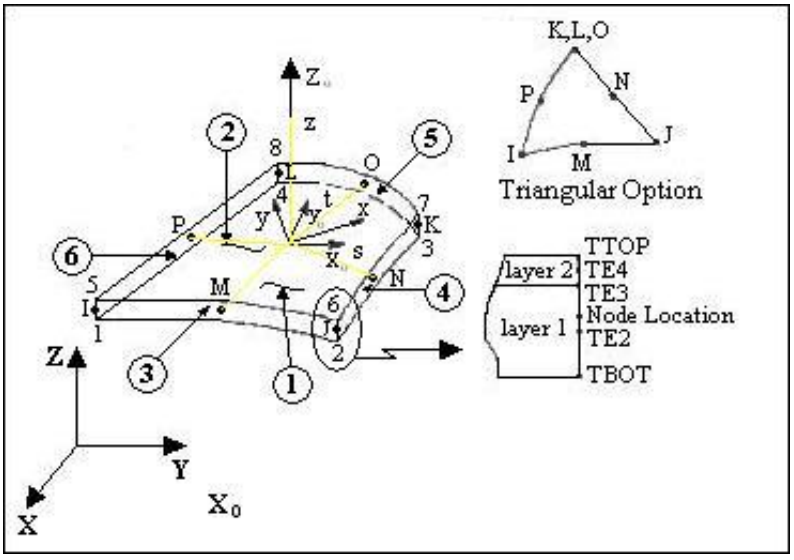

Fig. (2) SHELL 132 3-D thermal shell element.

RESULTS AND DISCUSSIONS

Table (2) estimates the verification test for composite laminate plate under different combined loadings of $(\upsilon_f = 25.076\%)$ for the plate having aspect ratio (1.8). The best case is (thermal cyclic + in-plane force N_{xx}) because the deflection is smaller than the other cases; but the percentage error in (thermal cyclic + in-plane force N_{xx}) and (thermal cyclic+ bending moment M_o + in-plane force N_{xx}) is not accurate because the (ANSYS 9) is the approximate solution. It can be shown the dynamic deflection decrease with the increasing of fiber volume fraction. The dynamic (Fortran 90) program is described in Fig. (3).

Table (2) Verification test for composite laminate plate under different combined loadings of $\upsilon_f = 25.076\%$.

Deflection (m)			
Deflection Field	CLPT	ANSYS Ver.9	Percentage Error (%)
Thermal Cyclic + Bending Moment M_o	-0.1777704 E-3	-0.18819 E-3	5.5367%
Thermal Cyclic + In-Plane Force N_{xx}	-0.7704258 E-6	-0.65088 E-6	15.5168%
Thermal Cyclic + Bending Moment M_o + In-Plane Force N_{xx}	-1.97185 E-5	-1.6735 E-5	15.1304%

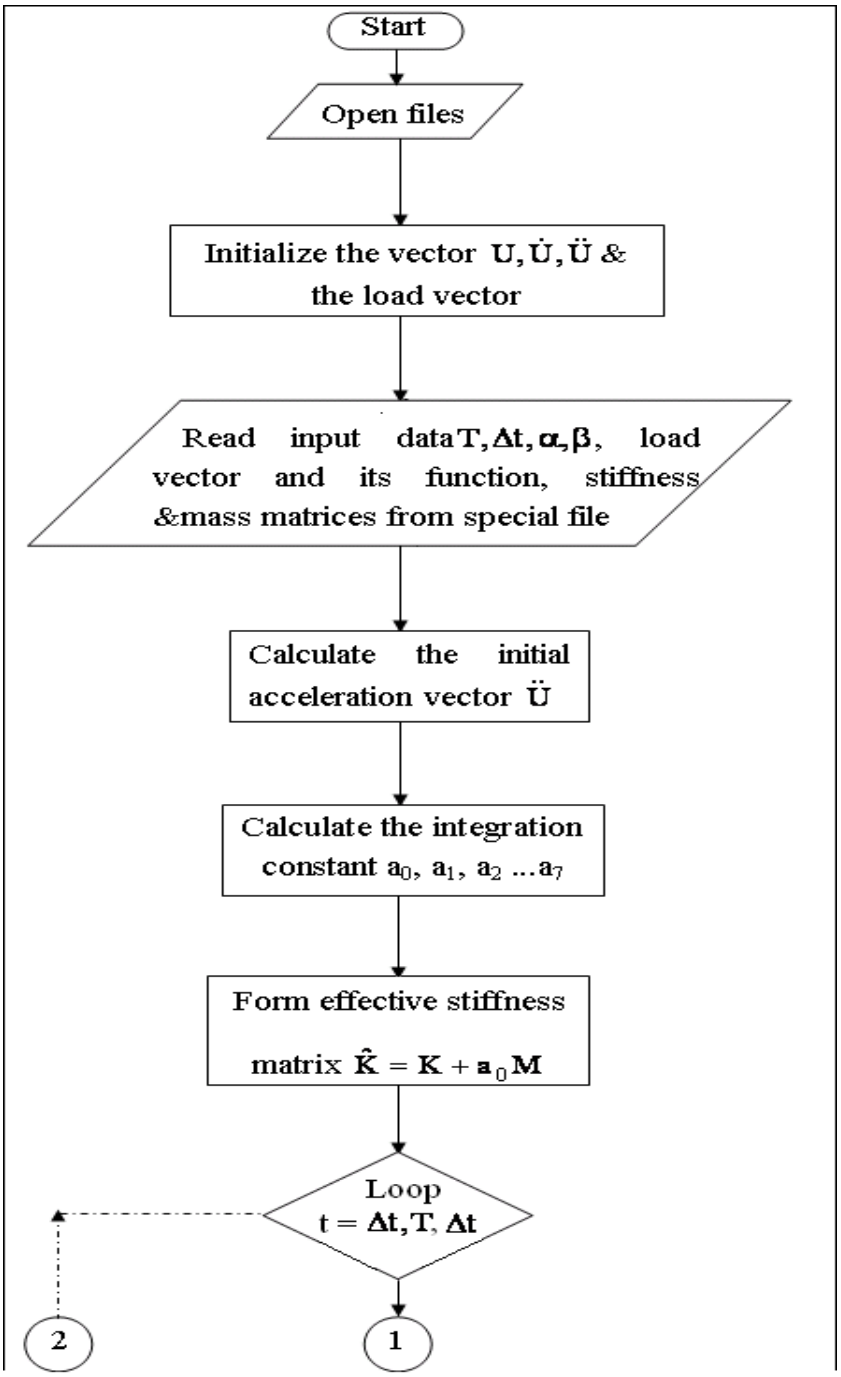
Start
Open files
Initialize the vector U, U̇, Ü & the load vector
Read input data T, Δt, α, β, load vector and its function, stiffness &mass matrices from special file
Calculate the initial acceleration vector Ü
Calculate the integration constant a_0, a_1, a_2 ... a_7
Form effective stiffness matrix $\hat{K} = K + a_0 M$
Loop
t = Δt, T, Δt
2
1

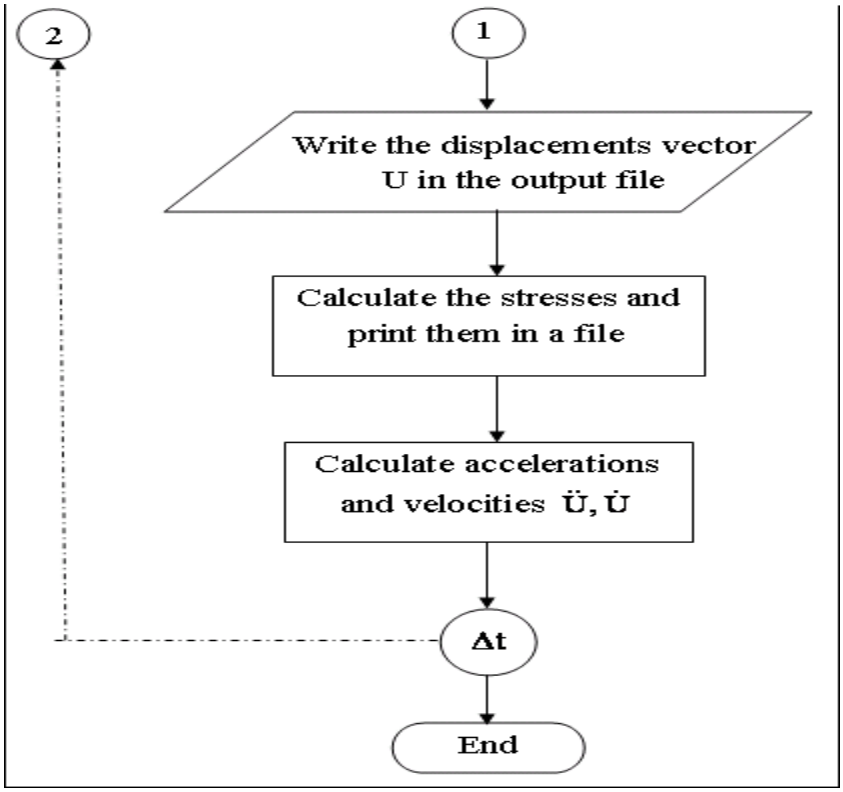

Fig. (3) Flow chart of the dynamic program, [Abdulla F.A. 2001].

Tables (3, 4, 5) show the effect of different fiber volume fractions and different loading percent of combined loading on deflection. In Tables (3, 5) the deflection can be decreased with the increasing of fiber volume fractions for all the increasing of loading percent; but the deflection can be increased with the increasing of loading percent for the same fiber volume fraction. In Table (3) the deflection still constant with the increasing of loading percent of combined loading for the same fiber volume fraction; but the deflection can be decreased with the increasing of fiber volume fractions.

Table (3) Effect of different fiber volume fractions and different load percents of (M_o) on deflection due to thermal cyclic + bending moment (M_o) of aspect ratio (a/b = 1.8).

Deflection (m) * 10^{-3}						
v_f % / Loading Percent of (M_o)	25.076%	40%	50%	60%	70%	80%
20%	-0.0379	-0.02876	-0.02393	-0.01964	-0.01562	-0.01176
40%	-0.07552	-0.05723	-0.04762	-0.03909	-0.03110	-0.02343
60%	-0.11308	-0.08570	-0.07131	-0.05855	-0.04658	-0.03511
80%	-0.15064	-0.11417	-0.09500	-0.07800	-0.06206	-0.04679
100%	-0.18819	-0.14264	-0.1187	-0.09746	-0.07754	-0.05846

Table (4) Effect of different fiber volume fractions and different load percents of (N_{xx}) on deflection due to thermal cyclic + in-plane force(N_{xx}) of aspect ratio (a/b = 1.8).

Deflection (m) * 10^{-6}						
υ_f %						
Loading Percent of (N_{xx})	25.076%	40%	50%	60%	70%	80%
20%	-0.65088	-0.48393	-0.39026	-0.3046	-0.22426	-0.14865
40%						
60%						
80%						
100%						

Table (5) Effect of different fiber volume fractions and different load percents of $(M_o \& N_{xx})$ on deflection due to thermal cyclic + bending moment(M_o) + in-plane force (N_{xx}) of aspect ratio (a/b = 1.8).

Deflection (m) * 10^{-4}						
υ_f %						
Loading Percent of $(M_o \& N_{xx})$	25.076%	40%	50%	60%	70%	80%
20%	-0.035661	-0.027356	-0.022759	-0.018561	-0.014572	-0.01063
40%	-0.068584	-0.052545	-0.043756	-0.035767	-0.028189	-0.02069
60%	-0.10151	-0.077733	-0.064753	-0.052973	-0.041805	-0.03075
80%	-0.13443	-0.10292	-0.085751	-0.07018	-0.055421	-0.040811
100%	-0.16735	-0.12811	-0.10675	-0.087386	-0.069038	-0.05086

Figs. (4, 5) show the convergence of dynamic central deflection with total degree of freedom. There is a small sudden change increasing in dynamic deflection occurring between numbers of degree-of-freedom (DOF) 81 and 2187 which then reached the steady-state case between numbers of degree-of-freedom (DOF) 2187 and 27783 for different fiber volume fractions for $(T_1 = 60°_C \text{ and } T_1 = -15\ °_C)$.

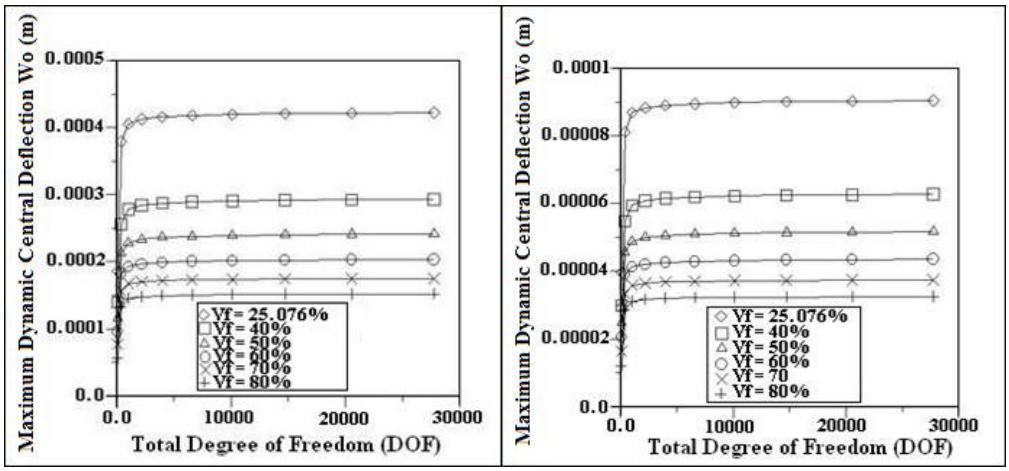

Fig. (4) Convergence of dynamic central deflection with total degree of freedom under $(T_1 = 60\ ^\circ_C)$.

Fig. (5) Convergence of dynamic deflection with total degree of freedom under $(T_1 = -15\ ^\circ_C)$.

Figs. (6, 7) give the convergence of dynamic load factor (D.L.F) with total degree of freedom. There is a large sudden change increasing in dynamic load factor occurring between numbers of degree-of-freedom (DOF) 81 and 14739 which then reached the steady-state case between numbers of degree-of-freedom (DOF) 14739 and 27783 for different fiber volume fractions for $(T_1 = 60^\circ_C$ and $T_1 = -15\ ^\circ_C)$. It can be noticed that the dynamic load factor decreased with the increasing of fiber volume fractions, while the fiber volume fractions increased with the increasing of fundamental natural frequency, then the dynamic load factor will be decreased.

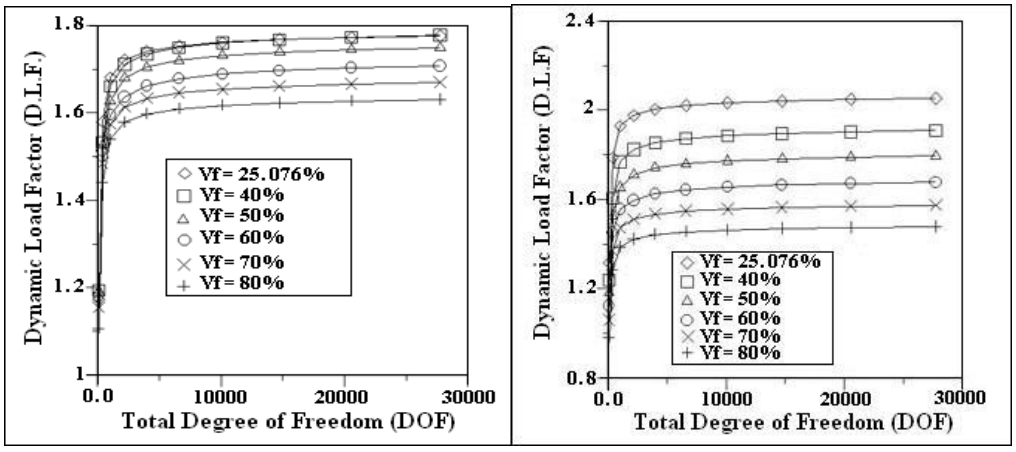

Fig. (6) Convergence of dynamic load factor with total degree of freedom under $(T_1 = 60\ ^\circ_C)$.

Fig. (7) Convergence of dynamic load factor with total degree of freedom under $(T_1 = -15\ ^\circ_C)$.

Figs. (8, 9) illustrate the effect of different fiber volume fractions on dynamic central deflection under thermal loadings ($T_1 = 60^\circ_C$ and $T_1 = -15\ ^\circ_C$) with time. Most of these curves reached to the steady-state case at time = 0.004 (settling time) and the dynamic deflection decreased with the increasing of fiber volume fractions. The best curve is the curve at fiber volume fraction ($\upsilon_f = 0.8$) because it reaches to the rise time first that is mean this curve has low value of rise time, settling time, and overshoot because increasing the fiber volume fractions causing increase in the value of fundamental natural frequency.

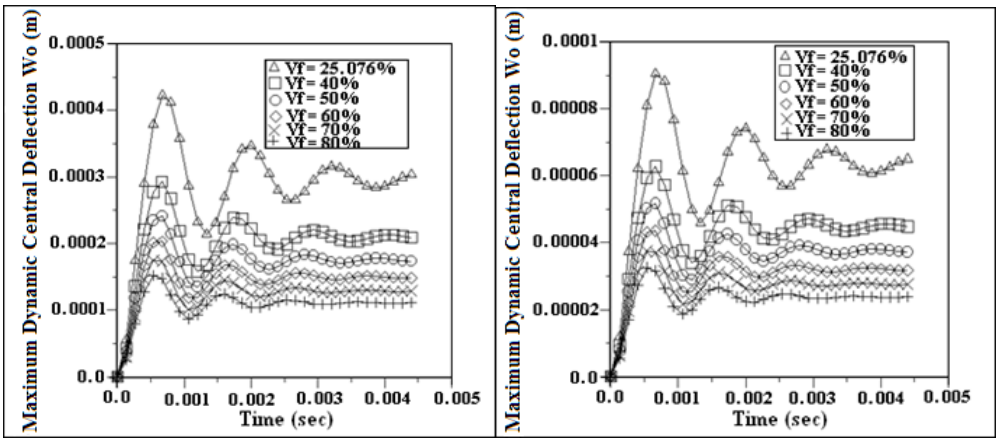

Fig. (8) Dynamic deflection variation with time under different fiber volume fractions of $(T_1 = 60\ ^\circ_C)$.

Fig. (9) Dynamic deflection variation with time under different fiber volume fractions $(T_1 = -15\ ^\circ_C)$.

Fig. (10) shows convergence of dynamic deflection with total degree of freedom under different combined loadings of $\upsilon_f = 25.076\%$ for simply supported plate with four edges. For the curve concern (thermal cycling + M_o) there is a large sudden change increasing in dynamic deflection occurring between numbers of degree-of-freedom (DOF) 390 and 4998 which then reached the steady-state case between numbers of degree-of-freedom (DOF) 4998 and 7686; but the curve concern (thermal cyclic + $M_o + N_{xx}$) there is a slow increasing of dynamic deflection occurring between numbers of degree-of-freedom (DOF) 390 and 1350 which then reached the steady-state case between numbers of degree-of-freedom (DOF)1350 and 7686. The curve concern (thermal cyclic + N_{xx}) there is no clear change in dynamic deflection with numbers of degree-of-freedom (DOF).

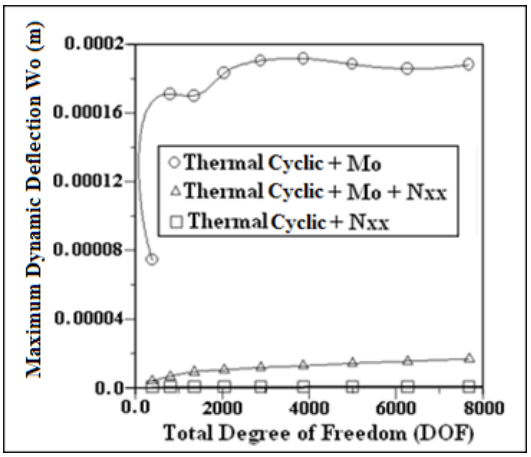

Fig. (10) Convergence of dynamic deflection with total degree of freedom under combined loadings of $(T_1 = -15\ ^{\circ}C)$.

Figs. (11, 12, 13) illustrate the effect of different fiber volume fractions on dynamic deflection with total degree of freedom for (thermal cyclic + M_o), (thermal cyclic + N_{xx}), and (thermal cyclic + $M_o + N_{xx}$) with a plate with aspect ratio (1.8) of simply supported plate with four edges; therefore the best curve is the curve of $v_f = 80\%$ for (thermal cyclic + N_{xx}) because this curve gives a small value of dynamic deflection equal to (0.22426 e-6).

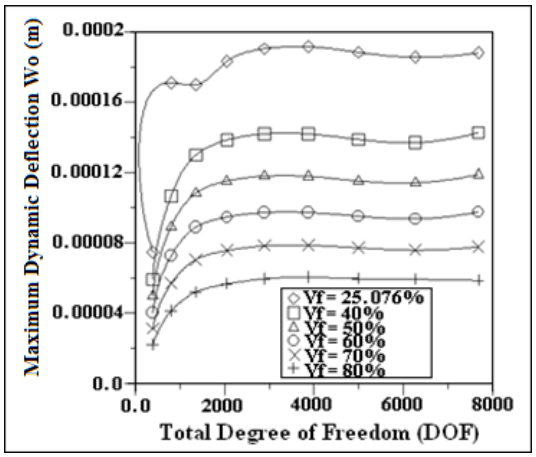

Fig. (11) Convergence of dynamic deflection with total degree of freedom under thermal cyclic + bending moment (M_o) for different fiber volume fractions.

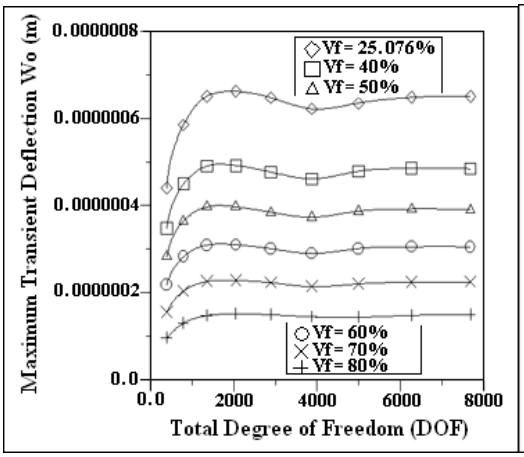

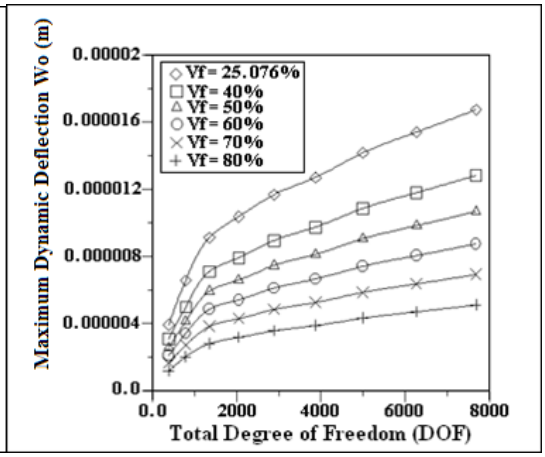

Fig. (12) Convergence of dynamic deflection with total degree of freedom under thermal cyclic + in-plane force (N_{xx}) for different fiber volume fractions.

Fig. (13) Convergence of dynamic deflection with total degree of freedom under thermal cyclic + bending moment (M_o) + in-plane force (N_{xx}) for different fiber volume fractions.

Fig. (14) shows comparisons between analytical solution (CLPT) and numerical solution (FEM) with the experimental published work [RayB.C.,2005] of $\upsilon_f = 25.076\%$ under thermal cyclic loading for the plate having aspect ratio (1.8) that concern inter-laminar shear stress varies with time. It can be noticed that the inter-laminar shear stress varies sinusoidal for both experimental and numerical solutions; but for analytical solution the inter-laminar shear stress reduced with time gradually because it applied via Levy solution on analytical part.

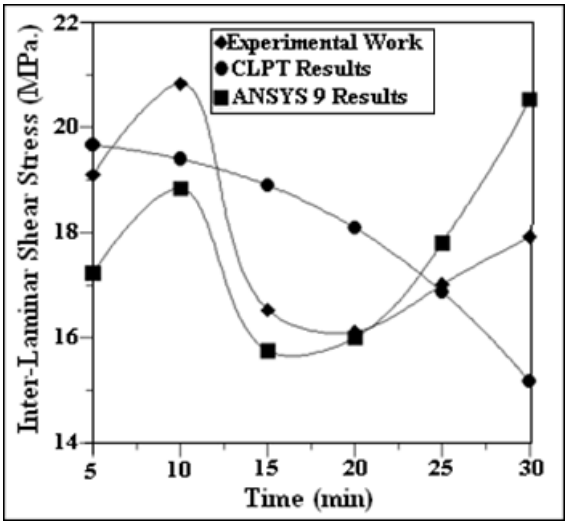

Fig. (14) Comparisons of inter-laminar shear stress varies with time under the effect of thermal cyclic of $\upsilon_f = 25.076\%$.

Fig. (15) gives the effect of different boundary conditions like (SSSS, CSSS, and CSCS) on inter-laminar shear stress varying with time of $\upsilon_f = 25.076\%$ using classical laminate plate theory (CLPT) for the plate having aspect ratio (1.8). The inter-laminar shear stress can be decreased with the increasing of time for all three curves; but the best curve that curve concern (CSCS) boundary condition this curve gives small value of inter-laminar shear stress because to reduce the mismatch between the thermal expansions of the resin and the fiber can be caused the thermal cyclic loading.

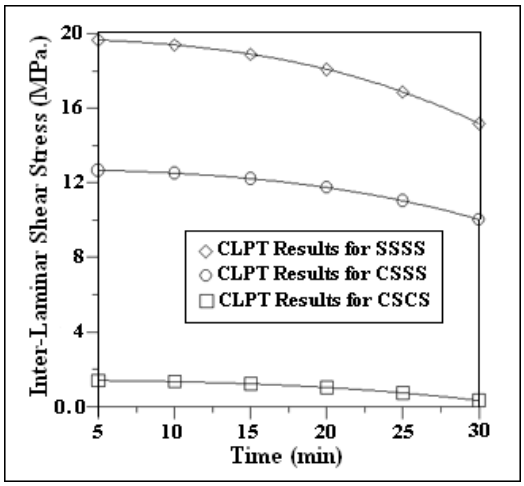

Fig. (15) Effect of different boundary conditions on inter-laminar shear stress varies with time of $\upsilon_f = 25.076\%$ under thermal cyclic loading.

Fig. (16) show the effect of different boundary conditions like (SSSS, CSSS, and CSCS) on central deflection varies with time of $\upsilon_f = 25.076\%$ using classical laminate plate theory (CLPT) for the plate having aspect ratio (1.8). The curve concern the boundary condition (SSSS) decreased with time; but the curve concern the boundary condition (CSSS, CSCS) have its value the minus sign because the particle's compression of composite laminate plate leads to concave upward occur in deflection direction due to this boundary condition. The conclusion of this minus sign the increasing of fixed or clamped edges gives increasing in concave upward instead of downward central deflection under thermal cyclic loading.

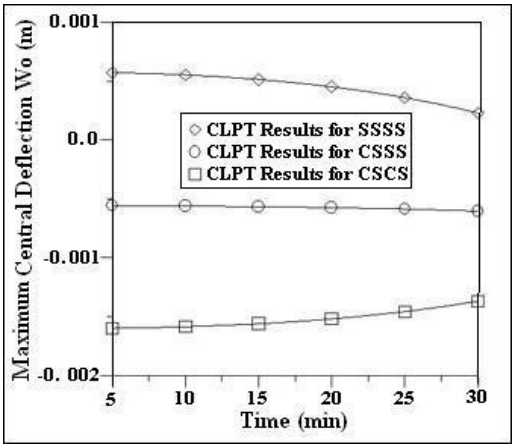

Fig. (16) Effect of different boundary conditions on central deflection varies with time of $\upsilon_f = 25.076\%$ under thermal cyclic loading.

Figs. (17, 18) illustrate the effect of different boundary conditions like (SSSS, CSSS, CSCS) on normal stresses in the (x, y) directions varies with time of $\upsilon_f = 25.076\%$ under thermal cyclic loading using classical laminate plate theory (CLPT) for the plate having aspect ratio (1.8). In the two figures, the curves have (SSSS, CSSS) boundary conditions that the normal stresses decreasing with the increasing of time because the most value of coefficient of thermal expansion decreased with time and that effect on the decreasing of normal stresses; but the positive sign of the value of normal stresses because of the case of the particle of composite laminate plate is tension due to these boundary conditions. The curve (CSCS) boundary condition casing decrease in the value of normal stress with time increasing; but the negative sign because of the particle of composite plate suffer from compression. The conclusion of these curves the increasing in the clamped or fixed edges causing increasing in particle's compression.

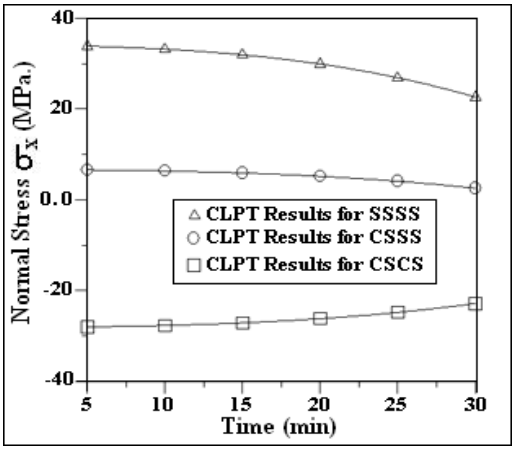

Fig. (17) Effect of different boundary conditions on normal stress (σ_x) varies with time of $\upsilon_f = 25.076\%$ under thermal cyclic loading.

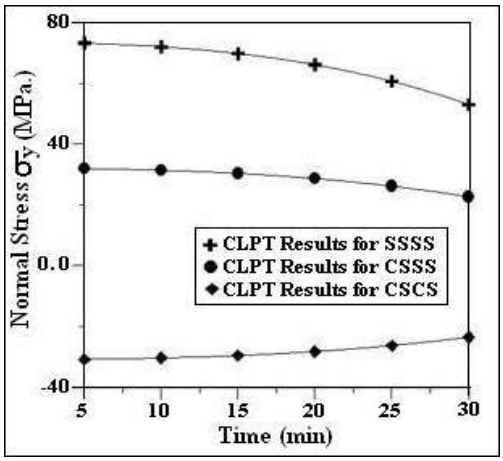

Fig. (18) Effect of different boundary conditions on normal stress (σ_y) varies with time of $\upsilon_f = 25.076\%$ under thermal cyclic loading.

Figs. (19, 20) show the effect of different boundary conditions on normal strain in the (x, y) directions varies with time of $\upsilon_f = 25.076\%$ under thermal cyclic loading using classical laminate plate theory (CLPT) for the plate having aspect ratio (1.8). The comment is the same as in Figs. (17, 18) because the stress is equal the multiplication of strain on material properties matrices and the positive, negative sign because the expansion and contraction on the particles of composite laminate plate.

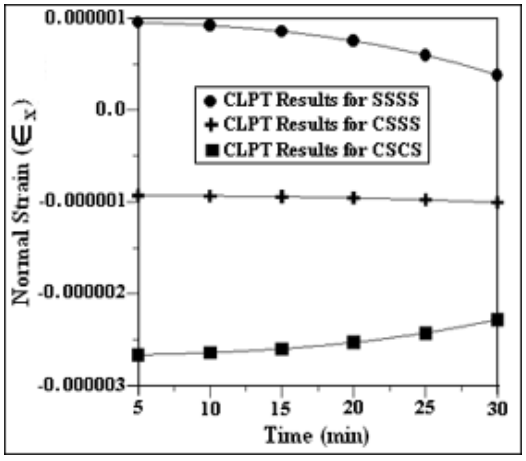

Fig. (19) Effect of different boundary conditions on normal strain (ε_x) varies with time of $\upsilon_f = 25.076\%$ under thermal cyclic loading.

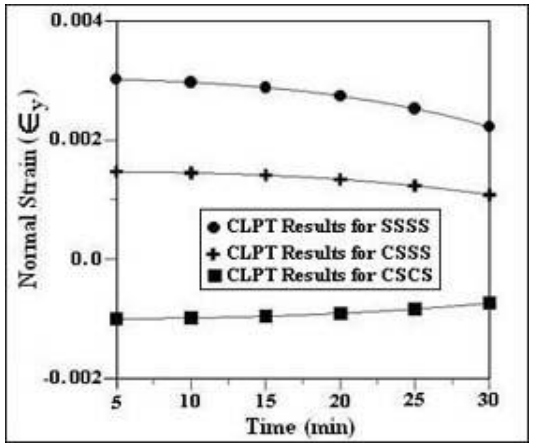

Fig. (20) Effect of different boundary conditions on normal strain (ε_y) varies with time of $\upsilon_f = 25.076\%$ under thermal cyclic loading.

CONCLUSIONS

This research conclude from its obtaining results under dynamic load (free vibration and dynamic response) of fiber-reinforced laminated plates comparing with analytical work, FEM and other investigations using different numerical and theoretical methods as follow :

- the maximum dynamic central deflection is decreased with the increasing of different fiber volume fractions of heating and cooling and that due to due to the increasing of the value of natural frequency (free vibration analysis) for both thermal loadings ($T_1 = 60°_C$ and $T_1 = -15\ °_C$).
- the increasing of fiber volume fractions causing decreasing in overshoot percent, rise time, and settling time; but all the plate with different fiber volume fractions have the same settling time and reached to the steady-state at the same time.
- The test of inter-laminar shear stress that the inter-laminar shear stress varies sinusoidal for both experimental, [3] and numerical solutions; but for analytical solution the inter-laminar shear stress reduced with time gradually.
- The effect of different percent of combined loadings and different fiber volume fractions on deflection. In the case of (thermal cyclic + M_o) and (thermal cyclic + $M_o + N_{xx}$) the deflection can be decreased with the increasing of fiber volume fractions for all the increasing of combined loadings percent; but the deflection can be increased with the increasing of loading percent for the same fiber volume fraction; but the deflection still constant with the increasing of loading percent of combined loading for the same fiber volume fraction for (thermal cyclic + N_{xx}).

REFERENCES

- Abdel A. Fabmy and Tbomas G. Cunningbam," Investigation of Thermal Fatigue in Fiber Composite Materials", National Aeronautics and Space Administration, WASHINGTON, July, 1976.

- B.C.Ray," Thermal Shock and Thermal Fatigue on Delamination of Glass Fiber Reinforced Polymeric Composites", Journal of Reinforced Plastics and Composites, Vol.24, No.1, 2005.

- B.C,RAY," Hydrothermal Shock Cycles on Shear Strength of Glass Fiber-Polyester Composites", Journal of Reinforced Plastics and Composites, Vol. 24, No. 12, 2005.

- B.C,RAY," Effect of thermal shock on interlaminar strength of thermally aged glass fiber reinforced epoxy composites", Journal of Applied Polymer Science, 2005.

- B.C.Ray," Hydrothermal Fatigue on Interface of Glass-Epoxy Laminates", Journal of Reinforced Plastics and Composites, Vol.24, No.10, 2005.

- B.C,RAY, " Loading rate sensitivity of glass fiber-epoxy composite at ambient and sub-ambient temperatures", Journal of Reinforced Plastics and Composites, 2005.

- B.C,RAY, "Effect of thermal shock on flexural modulus of thermally and cryogenically conditioned kevlar/epoxy composites", Journal of Advanced Composites Letters, Vol.14, No.2, 2005.

- Carlo A.Ginty and Christos C.Chamis," Hygrothermomechanical Fiber Composite Fatigue: Computational Simulation", NASA Technical Memorandum 100840, March, 1988.

- Fadhel Abbas Abdulla," Analysis of Composite Plate Subjected to Impact Load", M.Sc. Thesis, AL-Mustansiriyah University, Mechanical Engineering Department, March, 2001.

- J.N. Reddy," Mechanics of Laminated Composite Plates and Shells", Second Edition, 2004.

SYMBOLS

English Letters

a	Large Span of Rectangular Plate (Length)
b	Small Span of Rectangular Plate (Breadth)
CSSS	Plate Subjected To Clamped-Simply-Simply-Simply Supported Boundary Condition

CSCS	Plate Subjected To Clamped-Simply-Clamped-Simply Support Boundary Condition
h	Thickness of Rectangular Plate
ILSS	Inter-Laminar Shear Strength
M_o	Bending Moment Per Unit Length Applied In y-Direction Of The Plate
N_{xx}	In-Plane Direct And Shear Forces
$\overline{Q}_{ij}$	Transformed Reduced Stiffness Elements
SSSS	Plate Subjected To Simply-Simply-Simply-Simply Supported Boundary Condition
T_1	Gradient Uniform Temperature
u_o, v_o	Extensional Displacement Components In The 2-D Coordinate System
u, v, w	Displacement Components In The 3-D Coordinate System
w_o	Mid-Plane Deflection Along z-Direction
x, y, z	The Cartesian Coordinate System
z_k, z_{k+1}	Upper & Lower Lamina Surfaces Coordinates Along z-Direction

Greek Letters

$\alpha_x , \alpha_y , \alpha_{xy}$	Direct And Shear Coefficient Of Thermal Expansion Respectively
ΔT	Temperature Variation Through Laminate Thickness
θ	Orientation Angle From x-Axis
υ_f	Fiber Volume Fraction
$\begin{Bmatrix} \varepsilon_{xx} \\ \varepsilon_{yy} \\ \gamma_{xy} \end{Bmatrix}$	Cartesian Strain Vector
$\begin{Bmatrix} \sigma_{xx} \\ \sigma_{yy} \\ \sigma_{xy} \end{Bmatrix}$	Cartesian Stresses Field Vector